PAPER

Charge transfer in plasma assisted dry reforming of methane using a nanosecond pulsed packed-bed reactor discharge

Plasma Sci. Technol. **23** (2021) 064007 (8pp) https://doi.org/10.1088/2058-6272/abed30

Charge transfer in plasma assisted dry reforming of methane using a nanosecond pulsed packed-bed reactor discharge

Shuai ZHANG (张帅)[1,2], **Yuan GAO** (高远)[1], **Hao SUN** (孙昊)[1], **Zhe FAN** (范喆)[1,2] **and Tao SHAO** (邵涛)[1,2,*]

[1] Beijing International S&T Cooperation Base for Plasma Science and Energy Conversion, Institute of Electrical Engineering, Chinese Academy of Sciences, Beijing 100190, People's Republic of China
[2] University of Chinese Academy of Sciences, Beijing 100049, People's Republic of China

E-mail: st@mail.iee.ac.cn

Received 31 December 2020, revised 8 March 2021
Accepted for publication 9 March 2021
Published 6 April 2021

Abstract

This paper is aimed to investigate the effect of packing material on plasma characteristic from the viewpoint of charge transfer process. Both the charge accumulation and release processes in the dielectric barrier discharge reactor and packed-bed reactor were investigated by measuring voltage and current waveforms and taking ICCD images. The packing material was ZrO_2 pellets and the reactors were driven by a parameterized nanosecond pulse source. The quantity of transferred charges in the dielectric barrier discharge reactor was enhanced when decreasing pulse rise time or increasing pulse width (within 150 ns), but reduced when the gas gap was packed with pellets. The quantity of accumulated charges in the primary discharge was larger than the quantity of released charges in the secondary discharges in the dielectric barrier discharge reactor, but they were almost equal in the packed-bed reactor. It indicates that the discharge behavior has been changed from the view of charge transfer process once the gas gap was packed with pellets, and the ICCD images confirmed it.

Keywords: non-thermal plasma, packed-bed reactor, dry reforming, plasma catalysis, charge transfer

(Some figures may appear in colour only in the online journal)

1. Introduction

Plasma assisted CO_2 dry reforming CH_4 (DRM) is a promising approach to convert these two greenhouse gases into syngas by equation (1) [1]. Many non-thermal plasma technologies have been used for this process, but to-date, the majority of researches has been carried out using the dielectric barrier discharge (DBD) reactor [2]. In particular, it will lead to better conversion and energy efficiency when a DBD reactor works with packing materials (which is called packed-bed reactor) for DRM [3–7], hydrogenation of CO_2 [8, 9], CO_2 decomposion [10–12], contaminant removal [13–15] and so on. Most of these results show that the packing material enhances electron density, mean electron energy, as well as conversion and energy efficiency, although the residence time is shortened

$$CH_4 + CO_2 \rightarrow 2H_2 + 2CO,\ \Delta H^{\circ}_{298\,K} = 247\ \text{kJ mol}^{-1}. \quad (1)$$

However, the interaction between plasma and packing materials is a complicated process and far to understand. On one hand, the packing material will lead to the changes in discharge behavior and plasma chemical process. The physicochemical, surface and structure properties might exert impressive effects on the energy density, electrical field distribution, and breakdown mechanism. On the other hand, energetic particles in plasma could affect the properties of packing material, such as its morphology or catalytic activity. Some researches regarding the packed-bed reactor have been

* Author to whom any correspondence should be addressed.

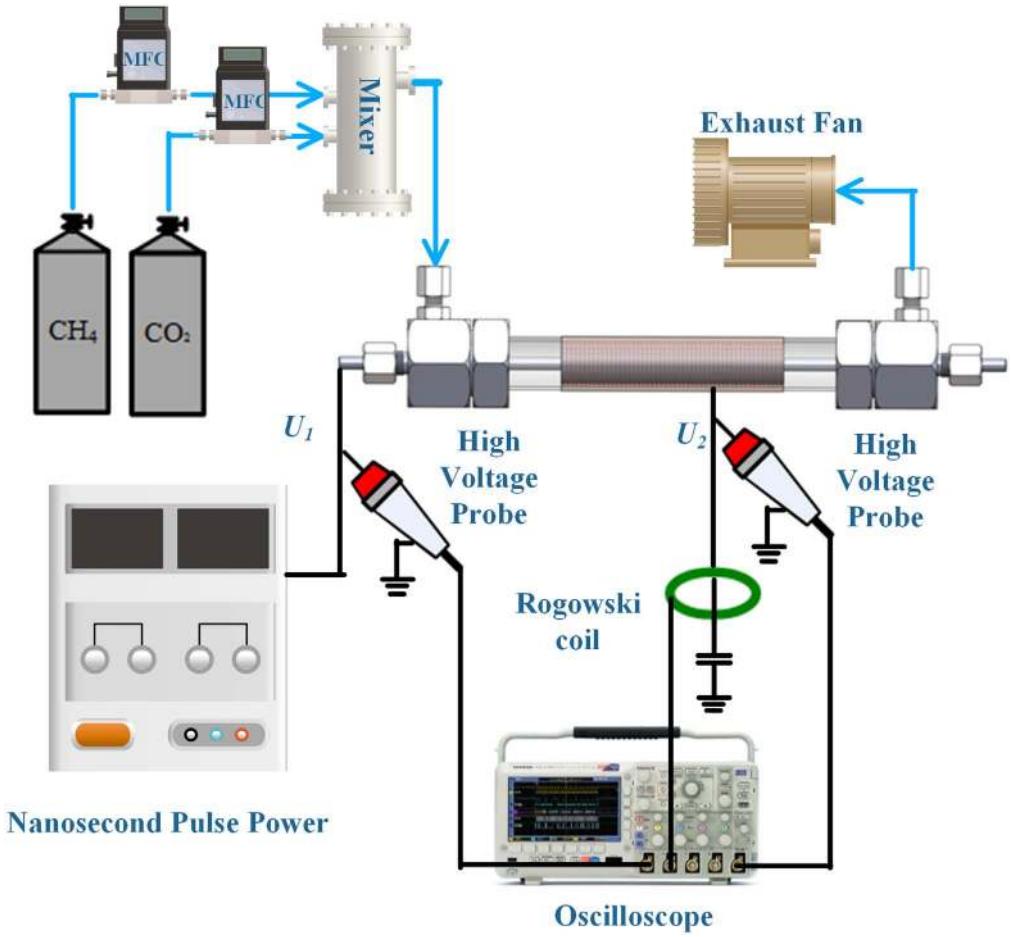

Figure 1. The schematic of experimental apparatus and packed-bed reactor.

conducted by scholars to investigate the synergic effect on plasma processing performance [16]. Tu *et al* [17] reported the typical filamentary discharge was converted to a combination of surface discharge and filamentary discharge when $BaTiO_3$ pellets were filled into the gas gap. Mei *et al* [18] and Xu *et al* [19] found that the presence of packing dielectric material would significantly enhance the mean electron energy. Van Laer *et al* [20, 21] and Wang *et al* [22] found that packing enhances the electric field strength and electron temperature from modelling research. Recently, nanosecond repetitively pulsed discharge has presented outstanding performance on the CO_2 dry reforming CH_4 process [23]. The nanosecond repetitive pulse can provide high density and energetic electrons, and also help for restraining the formation of thermal contraction in micro-discharge channels, which means that the interaction between plasma and packing materials in this type of discharge may be much different with the others [24–28]. Meanwhile, the wide adjustable ranges of pulse parameters can control the discharge process, making the intensive study of charge transferring characterization possible.

It has been reported that the packing materials have some influence on the plasma assisted conversion process under AC driven DBD plasma [17–22]. However, the conversion process may be not be exactly the same as that in the unipolar nanosecond pulsed DBD plasma, because the continuous charge accumulation during the previous pulse may restrain the discharge process of the next pulse. In this paper, an experimental research of plasma assisted CO_2 dry reforming CH_4 by a parameterized nanosecond pulse power gives an insight to the interaction between plasma and packing materials. The effect of packing materials on the charge transfer characterization is investigated by recording voltage and current waveforms and time-resolved luminescent images.

2. Experimental procedure

2.1. Experimental setup

Figure 1 shows the schematic of experimental setup. The reactors used a quartz tube as dielectric with outer diameter of 25.1 mm and wall thickness of 1.5 mm, a stainless steel rod as high voltage electrode with outer diameter of 17.6 mm and a 40 mm long indium-tin oxides film as ground electrode. The discharge volume of the DBD reactor was 5.6 ml with a gas gap of 2.25 mm, while the discharge volume was about 3.5 ml when filling with 1.2 mm diameter ZrO_2 pellets (45 wt.% ZrO_2, 40 wt.% Al_2O_3 and 15 wt.% SiO_2). The reactors was

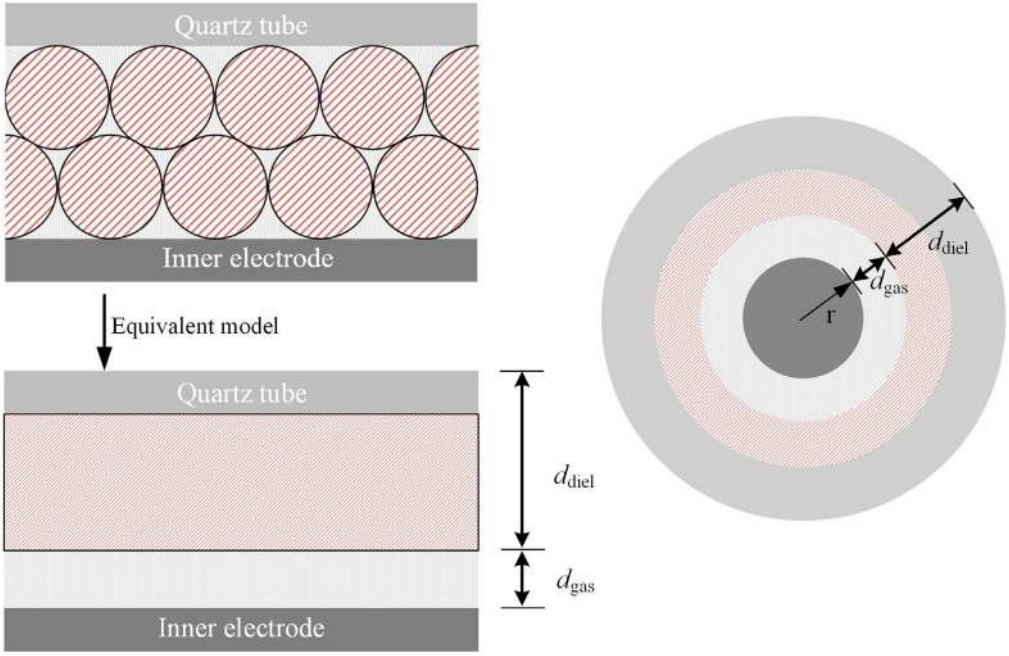

Figure 2. Equivalent electrical circuit model for the packed-bed reactor.

driven by a positive nanosecond pulse power source (Smart Maple HV-2015, China), which provides a maximum pulse voltage of 25 kV and a variable pulse repetition frequency up to 15 kHz. The pulse rise/fall time can be adjusted from 50 ns to 500 ns and the pulse width up to 1 ms. The voltage on the reactors was measured by a high voltage probe (Tektronix P6015, 1000:1, defined as U_1) and the current was detected with a Rogowski coil (Pearson 6595, 2:1), respectively. The voltage on the capacitor (1000 pF) was measured by another high voltage probe (Pin-tech P6010A, 100:1, defined as U_2). All the electrical signals were recorded by an oscilloscope (Tektronix DPO 2024). CH_4 and CO_2 were controlled through mass flow controllers (Sevenstar D07-19), respectively. It is worth noting that H_2 and CO are the major products. In addition, a small amount of light hydrocarbons were detected with gas chromatograph, such as C_2H_6, C_3H_8 and C_4H_{10}, as presented in our previous article [25]. The default electrical parameters include a pulse rise time of 200 ns, a pulse fall time of 200 ns, a pulse width of 200 ns, and the settled CO_2/CH_4 molar ratio of 1:1 was selected in our experiments.

2.2. Equivalent circuit model

Usually, an equivalent circuit of DBD in unipolar pulse excitation was introduced to estimate the electrical parameters [29]. As for the packed-bed reactor, the packing pellets could also be regarded as a dielectric and assumed to a circular tube that connected to the quartz tube [18, 19], as shown in figure 2. Here, the equivalent thicknesses of gas gap (d_{gas}) and dielectric (d_{diel}) of the packed-bed reactor could be estimated from the volume of packing pellets.

Table 1. Estimated equivalent capacitances of the DBD and packed-bed reactors.

Item	d_{gas} (mm)	ε	C_{diel} (pF)	C_{gas} (pF)	C_{cell} (pF)
DBD reactor	2.25	1	64.7	9.8	8.5
Packed-bed reactor	1.2	18	53.5	22.7	15.1

The capacitance of dielectric (C_{diel}) and the gas gap (C_{gas}) can be calculated by equation (2):

$$C = \frac{2\pi\varepsilon_0\varepsilon l}{\ln(R_x/r_x)} \tag{2}$$

where ε_0 and ε are relative permittivity of vacuum and packing pellets. R_x and r_x represent an equivalent external diameter and inner diameters of the capacitor (dielectric or the gas), respectively. For example, R_x and r_x for calculation of C_{diel} of the packed-bed reactor are as follows:

$$R_x = r + d_{gas} + d_{diel} \tag{3}$$

$$r_x = r + d_{gas} \tag{4}$$

where r is the radius of the center electrode. The results are shown in table 1, where C_{diel}, C_{gas}, C_{cell} represent the capacitances of dielectric, gas gap and the entire reactor, respectively.

3. Result and discussion

3.1. Electrical characteristic

The typical discharge voltage and current waveforms were investigated, as shown in figure 3, with an illustration of discharge images. It is common that there were two main discharge processes for both DBD and packed-bed reactors,

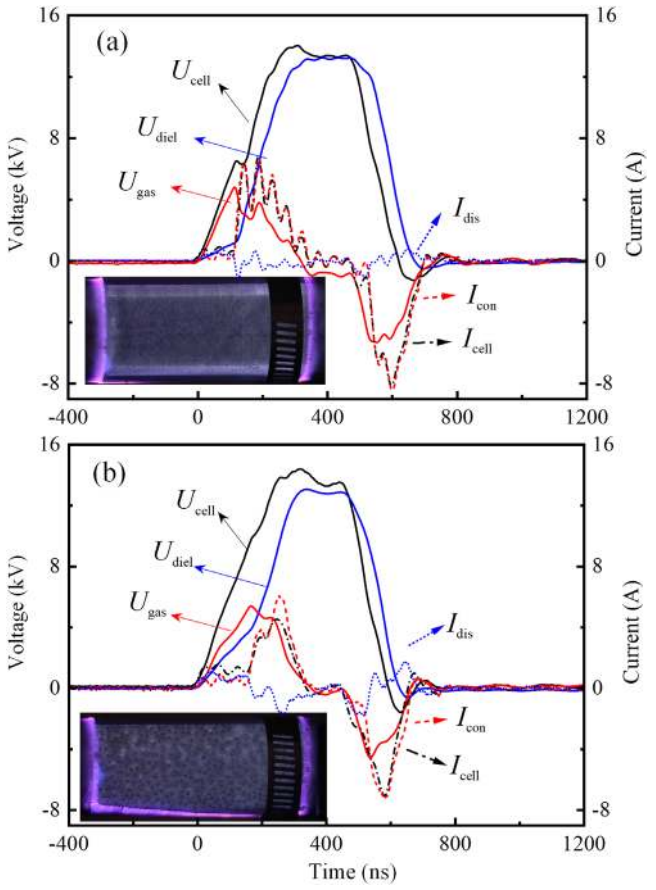

Figure 3. Typical discharge characteristics of (a) DBD reactor and (b) packed-bed reactor under nanosecond repetitive pulses.

i.e. primary discharge at pulse rise time because of external electric field and secondary discharge at pulse fall time on account of reverse electric field resulting from the accumulated charge on the dielectric surface, respectively. The current peaks of the discharge current (I_{cell}) in DBD reactor can reach to about 6.8 A at pulse rise time and −8.4 A at pulse fall time, while the current peaks of I_{cell} were smaller and appeared a dozen of nanoseconds later when packing ZrO_2 pellets.

The voltage over gas gap (U_{gas}) and dielectric (U_{diel}), along with the conduction current (I_{con}) and displacement current (I_{dis}) were calculated according to equations (5)–(9), as shown in figure 3

$$U_{diel} = (1/C_{diel})\int I_{cell}\,dt + U_{cell}(t_0) \tag{5}$$

$$U_{gas} = U_{cell} - U_{diel} \tag{6}$$

$$\frac{U_{gas}}{U_{diel}} \approx \frac{C_{diel}}{C_{gas}} \tag{7}$$

$$I_{con} = \frac{dU_{gas}(t)}{dt} \tag{8}$$

$$I_{dis} = I_{cell} - I_{con}. \tag{9}$$

One characteristic of the results is that the U_{gas} peak was about 4.5 kV, but U_{diel} peak was almost equal to applied voltage (U_{cell}) peak in the DBD reactor. As for packing ZrO_2 pellets, U_{gas} peak increased and U_{diel} peak decreased a bit. I_{con} was almost equal to I_{cell} while I_{dis} was very small. I_{con} reduced and I_{dis} was enhanced because of the presence of ZrO_2 pellets. It indicates that mostly power energy would be deposited on the dielectric, with slight improvement when packing ZrO_2 pellets. Another one is that, there were multi-current peaks at the pulse rise time for the DBD reactor, which means that the discharge may be a uniform one. A similar phenomenon has been reported by Mangolini *et al* [30] and Yang *et al* [31]. On the contrary, there was only one current peak at the pulse rise time for the packed-bed reactor.

Figure 4 shows the effects of pulse fall time on U_{diel} and U_{gas} in the DBD and packed-bed reactors, respectively. Here, we tested the pulse fall time from 100 ns to 500 ns with pulse rise time of 200 ns and pulse width of 200 ns. From figure 4(a), it is found that U_{gas} and U_{diel} changed slightly at the period of pulse rise time and pulse width. However, due to the introduction of packing pellets, U_{diel} decreased dramatically at the period of pulse width as increasing the pulse fall time, as shown in figure 4(b). Charge transfer process might contribute a lot to the above difference. The descending of U_{diel} means the enhancement of C_{diel} or the reduction of C_{gas} according to equation (6).

3.2. Charge characteristic

As mentioned above, the secondary discharge is a result of charge accumulation on the gas gap. In this section, we check the charge accumulation process under different pulse rise times and pulse widths, in which the quantity of transferred charges through the reactor (Q_{cell}), the gas (Q_{gas}) and the dielectric (Q_{diel}) were calculated according to equations (10)–(12), respectively

$$Q_{cell} = \int I_{cell} \times dt \tag{10}$$

$$Q_{gas} = \int I_{con} \times dt \tag{11}$$

$$Q_{diel} = \int I_{dis} \times dt. \tag{12}$$

Figure 5 presents the influences of pulse rise time and pulse width on the charge transition behavior in the DBD reactor. Commonly, the growing pulse width could enhance the charge accumulation on dielectric surface, but a saturation point of charge accumulation can be obtained with a long enough pulse width. It is found that the accumulated Q_{gas} and Q_{cell} reach their saturation points at a pulse width of about 150 ns under different pulse rise times in figures 5(a) and (b). On the other hand, the saturated Q_{gas} and Q_{cell} clearly decrease with the increase of pulse rise time.

However, figure 5(c) shows that Q_{diel} was observed to continuously increase with ascending pulse width under different pulse rise times. The continuous growth of Q_{diel} with a longer pulse width may increase the energy loss on dielectric, an appropriate pulse width and rising time are crucial to

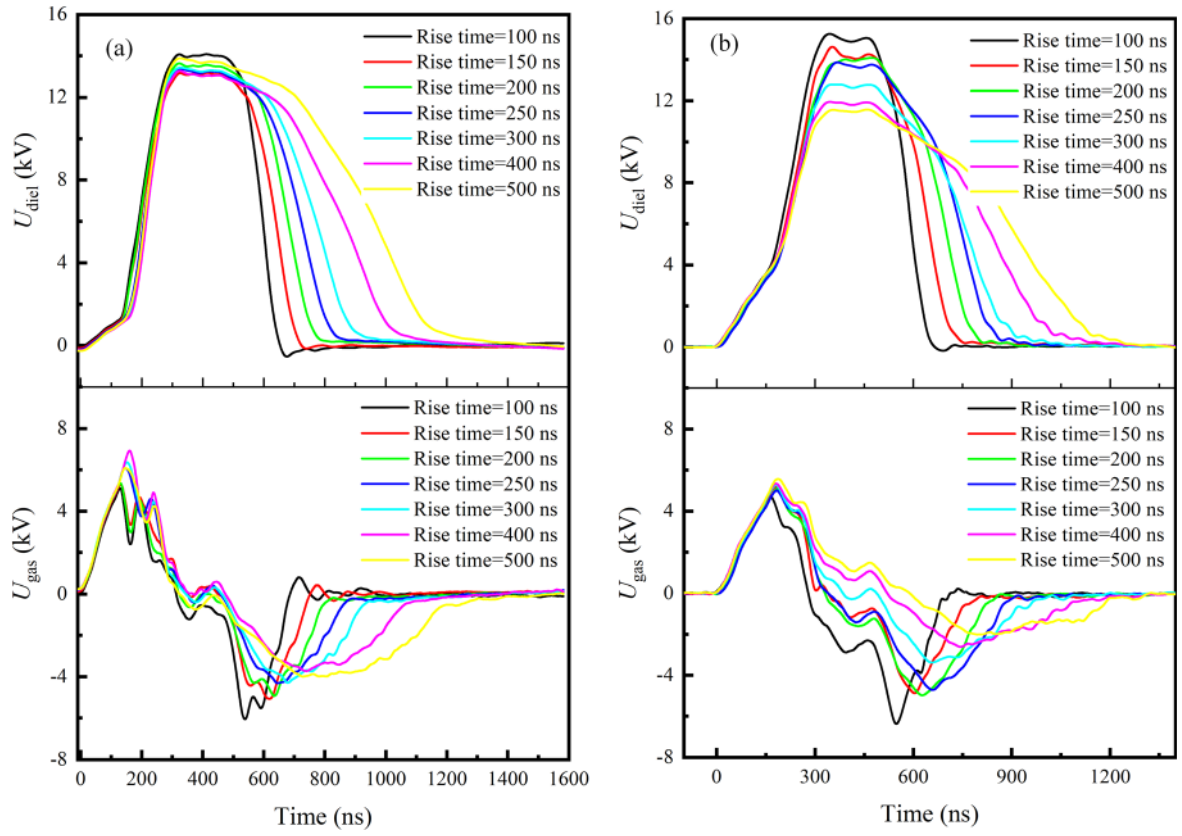

Figure 4. Effect of pulse fall time on U_{gas} and U_{diel} of (a) DBD reactor and (b) packed-bed reactor.

improve the energy efficiency. To study the secondary discharge, it is reasonable to choose the pulse rise time of 200 ns and pulse width of 200 ns for studying the charge accumulation and release processes in the next section.

3.2.1. Accumulation process. The charge accumulation process and release process happen during the whole discharge period. However, it is reasonable to regard that the main charge accumulation process happens in the primary discharge while the main charge release process happens at the secondary discharge. Here, we defined the beginning of pulse rise time as t_0, the medial point of pulse width as t_1, and the end of pulse fall time as t_2. The quantity of accumulated charges in the primary discharge ($Q_{primary}$) can be calculated by equation (13)

$$Q_{primary} = \int_{t_0}^{t_1} I_{con} \times dt. \quad (13)$$

Figure 6 shows the variation of $Q_{primary}$ of the DBD and packed-bed reactors under different pulse rise times and pulse widths. It is shown that the $Q_{primary}$ also increased almost linearly when increasing the pulse width from 0 ns to ~100 ns and then changed a little when the pulse width further grew. Moreover, the $Q_{primary}$ decreased distinctly when increasing the pulse rise time whether the DBD reactor or packed-bed reactor. The variation was the same as Q_{gas} and Q_{cell} in figures 5(a) and (b) since that the charge accumulation process was the dominant factor in the whole transfer process. However, the $Q_{primary}$ in the packed-bed reactor was always smaller than that in the no packing cases at all the pulse rise times and pulse widths, compared the figures 6(a) and (b).

3.2.2. Release process. The pulse fall time has little impact at the period of pulse rise time, but a non-ignorable impact at the period of pulse width on the charge accumulation process. Next, the charge accumulation and release processes under different pulse fall times have been investigated, as shown in figure 7. The quantity of released charges in the secondary discharge ($Q_{secondary}$) can be calculated by equation (14)

$$Q_{secondary} = \int_{t_1}^{t_2} I_{con} \times dt. \quad (14)$$

Firstly, it is striking that the quantities of accumulated and released charges ($Q_{primary}$ and $Q_{secondary}$) in the DBD reactor were clearly larger than those in the packed-bed reactor. Then, the $Q_{primary}$ and $Q_{secondary}$ in the packed-bed reactor declined faster than those in the DBD reactor as the pulse fall time increased.

Here, if we defined ΔQ as the difference between $Q_{primary}$ and $Q_{secondary}$:

$$\Delta Q = Q_{primary} - Q_{secondary}. \quad (15)$$

Usually, in a fast pulsed DBD reactor, residual charges (Q_{res}) before the application of pulse voltage cannot be ignored [32],

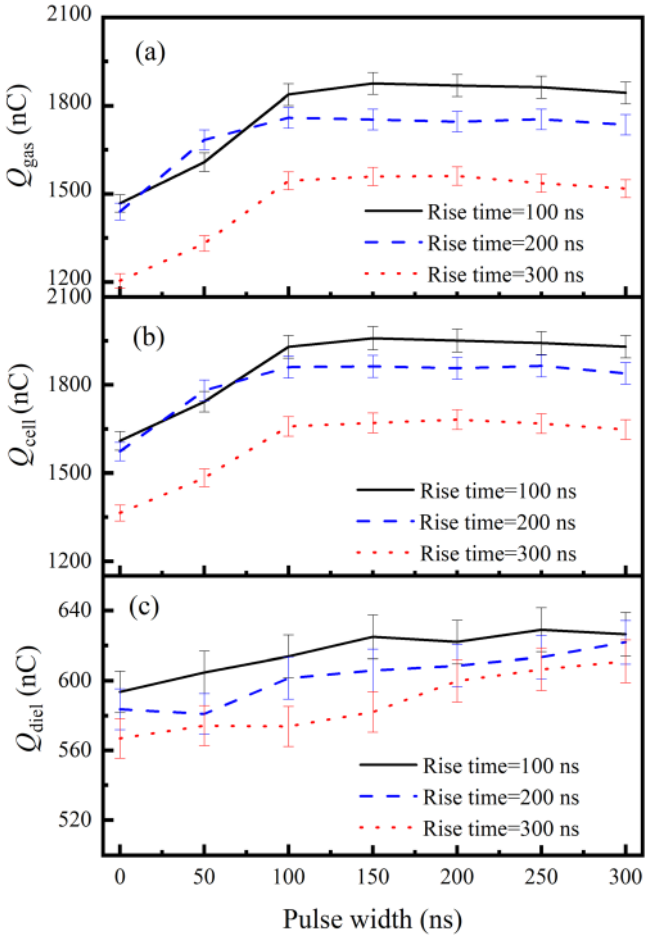

Figure 5. The variation of charge (a) $Q_{gas,}$ (b) Q_{cell} and (c) Q_{diel} in the DBD reactor.

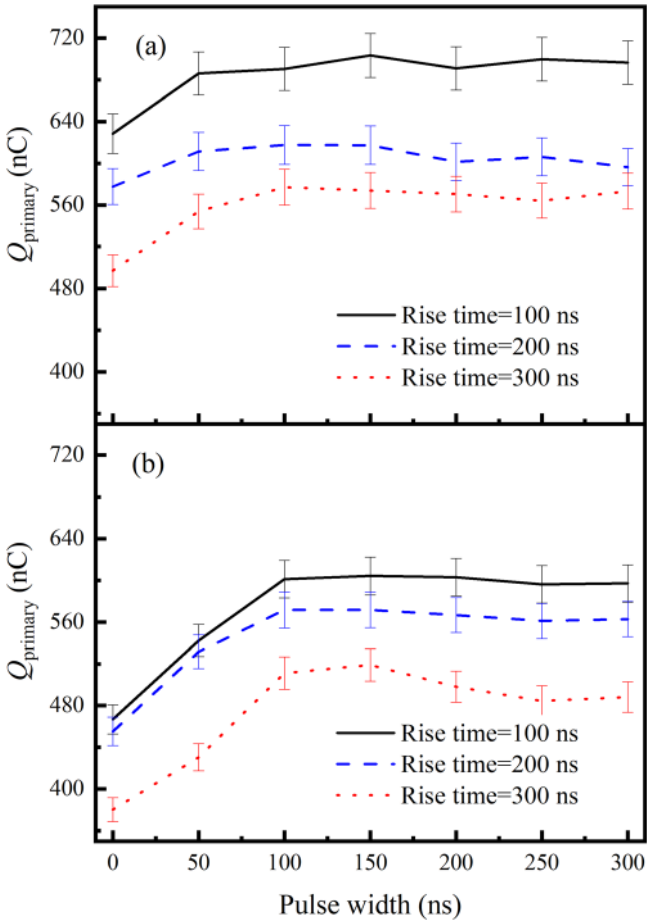

Figure 6. The variation of $Q_{primary}$ of the (a) DBD reactor and (b) packed-bed reactor.

as shown in equation (16)

$$Q_{cell} + Q_{res} = \int I_{cell} \times dt. \tag{16}$$

Of course, ΔQ is not Q_{res} because there may be dissipated charges ($\Delta Q - Q_{res}$) during the long time interval of two pulses. In fact, the dissipation rate is closely related to ΔQ [33]. If a dissipation rate (η) was defined, the relationship between ΔQ and Q_{res} is:

$$Q_{res} = (1 - \eta) \times \Delta Q. \tag{17}$$

Hence, it is reasonable to draw a conclusion that the variation tendency of Q_{res} is consistent with ΔQ when changing the pulse parameters.

Finally, it is meaningful that $Q_{primary}$ kept approximately equal to $Q_{secondary}$ in the packed-bed reactor while the difference between $Q_{secondary}$ and $Q_{primary}$ became larger in the DBD reactor when increasing the pulse fall time. The reason may be that the gas gap reduces significantly and becomes easy to breakdown, hence the charges were easy to release in the packed-bed reactor. The result indicates that there is no Q_{res} from the previous discharge period to participate into the next discharge period in the packed-bed reactor, but abundant residual charges will participate in the

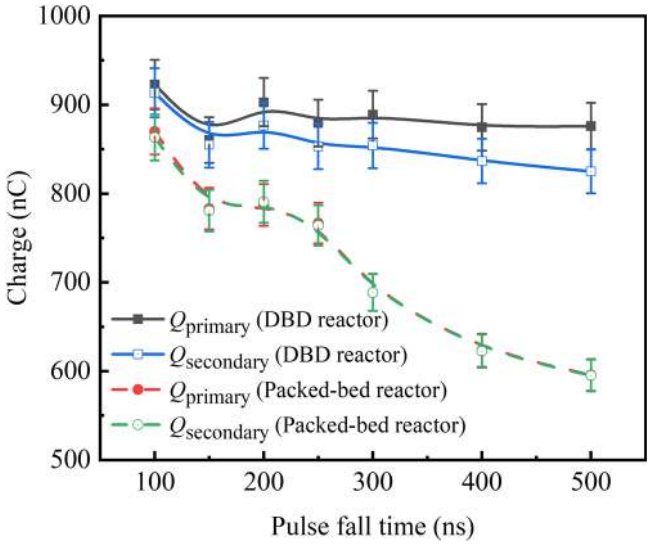

Figure 7. The variation of $Q_{primary}$ (solid symbol) and $Q_{secondary}$ (hollow symbol) in the DBD reactor (solid line) and the packed-bed reactor that packing with ZrO_2 (dash line).

next discharge period in the DBD reactor as increasing the pulse fall time. Thus it can be seen that it is beneficial to reduce residual charges and the breakdown voltage in the discharge period under unipolar pulse voltage by packing

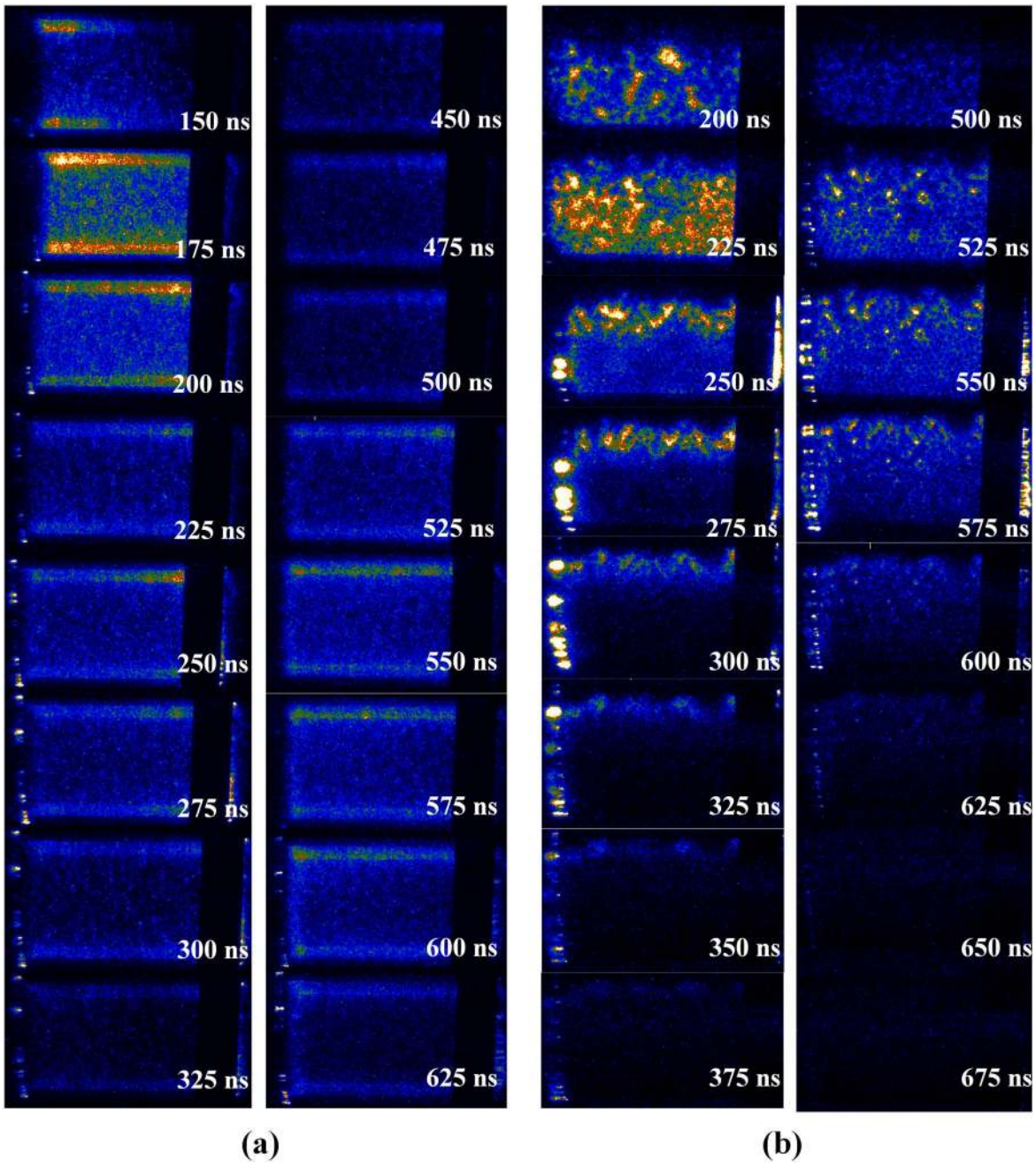

Figure 8. The time-resolved discharge evolution of the (a) DBD reactor and (b) packed-bed reactor.

ZrO_2 pellets. On the other hand, the charge decrease rate is also different between the DBD reactor and the packed-bed reactor when the pulse fall time increases. Both $Q_{primary}$ and $Q_{secondary}$ of the DBD reactor are always higher and decrease more slowly than those of the packed-bed reactor. The reason may be attributed to the memory effect of residual charges is more remarkable in the DBD reactor, compared with the packed-bed reactor.

3.3. Discharge evolution

Here, an ICCD camera can be used to record the time-resolved discharge evolution process. Figure 8 shows the successive discharge behavior of the DBD reactor and packed-bed reactor, with the pulse voltage of 13 kV and pulse repetition frequency of 3 kHz. The ICCD setting is a gain of 2500, gate delay step of 50 ns, gate width of 25 ns and gate width step of 0 ns. It found that the discharge appeared in the whole reactor both in the primary and secondary discharges for the DBD reactor, but it turned to a volume and surface combined discharge when packing ZrO_2 pellets. In addition, the discharge duration in the fall time become very short when packing ZrO_2 pellets. It is a good evidence for the phenomenon in section 3.2.2.

There is no doubt that the discharge with packing dielectric materials should be more uniform than that without packing in an alternating current (AC) DBD plasma [34]. At atmospheric pressure, it is the fact that the AC DBD plasma is usually

non-uniform (i.e. brightly filamentous) if feeding gas is not a noble gas. When the gas gap is packed by dielectric pellets, the residual charges nearby the surface of the dielectric pellets will form surface discharge. Hence, it looks more uniform in the case of packing dielectric materials. In contrast, the discharge morphology will be different when the high voltage power source is a nanosecond pulse power source. The discharge usually seems uniform in a nanosecond pulsed DBD reactor. When the gas gap is packed by dielectric pellets, the discharge area is separated and surface discharge is enhanced, which will lead to the diversification of discharge intensity.

4. Conclusion

The electrical and charge transfer characteristics of CO_2 reforming of CH_4 were studied in the dielectric barrier discharge and packed-bed reactors. Typical voltage and current waveforms and ICCD images were recorded under different pulse parameters. It is shown that the discharge current peaks became smaller and appeared a dozen of nanoseconds later, and the voltage over dielectric decreased dramatically at the period of pulse width for the packed-bed reactor as increasing the pulse fall time. The quantity of transferred charges reaches a saturation point when pulse width is increased to 150 ns, and reduces with the increase of pulse rise time or packing ZrO_2 pellets. Moreover, the accumulated charges in the primary discharge were more than the released charges in the secondary discharge, but they were always equal in the packed-bed reactor as increasing the pulse fall time, which would be a result of the decrease in gas gap and the reduction of breakdown voltage. The ICCD images indicate that it is a relatively uniform volume discharge in the DBD reactor, but turns to a volume and surface combined discharge when packing ZrO_2 pellets.

Acknowledgments

This work was supported by the National Science Fund for Distinguished Young Scholars (No. 51925703), National Natural Science Foundation of China (Nos. 51637010, 51707186 and 51807190).

References

[1] Lavoie J M 2014 *Front. Chem.* **2** 81
[2] Tao X M *et al* 2011 *Prog. Energ. Combust. Sci.* **37** 113
[3] Tu X *et al* 2011 *J. Phys. D: Appl. Phys.* **44** 274007
[4] Wang L *et al* 2017 *Angew. Chem.* **56** 13679
[5] Hu J *et al* 2016 *Plasma Sci. Technol.* **18** 254
[6] Ray D, Chawdhury P and Subrahmanyam C 2020 *ACS Omega* **5** 14040
[7] Chung W C *et al* 2014 *Energ Fuel* **28** 7621
[8] Gao Y *et al* 2020 *Chem. Eng. J.* 127693
[9] Xu W W *et al* 2019 *Plasma Sci. Technol.* **21** 044004
[10] Ray D *et al* 2021 *J. CO_2 Util.* **44** 101400
[11] Ray D, Chawdhury P and Subrahmanyam C 2020 *Environ. Res.* **183** 109286
[12] Zhu S J *et al* 2019 *Plasma Sci. Technol.* **21** 085504
[13] Zhu B *et al* 2019 *Plasma Sci. Technol.* **21** 115503
[14] Chawdhury P *et al* 2021 *Appl. Catal. B: Environ.* **284** 119735
[15] Wang Y *et al* 2021 *J. Hazard. Mater.* **404** 123965
[16] Kim H H, Kim J H and Ogata A 2009 *J. Phys. D: Appl. Phys.* **42** 135210
[17] Tu X, Gallon H J and Whitehead J C 2011 *IEEE Trans. Plasma Sci.* **39** 2172
[18] Mei D H *et al* 2014 *Plasma Sources Sci. Technol.* **24** 015011
[19] Xu S J *et al* 2018 *Plasma Sources Sci. Technol.* **27** 075009
[20] Van Laer K and Bogaerts A 2017 *Plasma Process. Polym.* **14** 1600129
[21] Van Laer K and Bogaerts A 2017 *Plasma Sources Sci. Technol.* **26** 085007
[22] Wang W Z *et al* 2018 *Chem. Eng. J.* **334** 2467
[23] Scapinello M, Martini L M and Tosi P 2014 *Plasma Process. Polym.* **11** 624
[24] Shao T *et al* 2018 *High Volt.* **3** 14
[25] Wang X L *et al* 2019 *Appl. Energy* **243** 132
[26] Xu Y F *et al* 2020 *Plasma Sci. Technol.* **22** 055403
[27] Huang B D *et al* 2020 *Chem. Eng. J.* **396** 125185
[28] Jiang N *et al* 2017 *J. Phys. D: Appl. Phys.* **50** 155206
[29] Shao T *et al* 2008 *J. Phys. D: Appl. Phys.* **41** 215203
[30] Mangolini L *et al* 2002 *Appl. Phys. Lett.* **80** 1722
[31] Yang D Z *et al* 2013 *Appl. Phys. Lett.* **102** 194102
[32] Zhang C *et al* 2017 *J. Phys. D: Appl. Phys.* **50** 405203
[33] Pipa A V *et al* 2012 *Rev. Sci. Instrum.* **83** 075111
[34] Wang Y B *et al* 2019 *ACS Catal.* **9** 10780